Macromolecules
ARTICLE

Macromolecules **2009**, *42*, 5811–5817 **5811**
DOI: 10.1021/ma9008934

One-Pot Synthesis of Thermoresponsive PNIPAM Hydrogel Microcapsules Designed to Function in Apolar Media

Marta Horecha, Volodymyr Senkovskyy,* Manfred Stamm, and Anton Kiriy*

Leibniz-Institut für Polymerforschung Dresden e.V., Hohe Strasse 6, 01069 Dresden, Germany

Received April 24, 2009; Revised Manuscript Received June 5, 2009

ABSTRACT: Poly(*N*-isopropylacrylamide) (PNIPAM) hydrogel microcapsules having a hydrophobic corona (MCs) were prepared by precipitation−polymerization performed in water-in-oil emulsion using polyethyleneoxide−polyisoprene block copolymer as macromolecular surfactant and a corona-forming compound. The resulting hydrogel MCs form stable dispersions even in highly apolar organic solvents, such as cyclohexane, but flocculate in water. An approach to load the MCs with water, based on addition of aqueous solutions to the dispersion of the MCs in THF followed by addition of apolar solvents to induce segregation of a water-rich phase, was developed. The water-filled hydrogel MCs show a well-pronounced swelling/deswelling transition triggered by temperature in an environment that contains only minute amounts of water. Encapsulating capabilities of the MCs were also demonstrated. The MCs can be envisaged for applications that require controlled dispersion and release of hydrophilic species in oils.

Introduction

Polymer microcapsules (MCs) attract a great attention due to their applications in drug delivery,[1] food technology, catalysis,[2] cosmetics, sensing,[3] photonics,[4] for encapsulation of dyes, inks, and pesticides, or utilizations as containers for confined chemical reactions.[5] Templating against hard (solid) templates, such as layer-by-layer self-assembly of desired materials onto preformed colloidal particles followed by core removal, is one of the most common methods for preparation of hollow structures.[6] This approach, however, has several intrinsic disadvantages, ranging from the inherent difficulty of achieving high product yields from the multistep synthetic process to the lack of structural robustness of the shells upon template removal. Still another disadvantage of this method is that refilling the hollow interior with functional species is also challenging. In a view of these difficulties, among many other approaches to hollow structures,[7] emulsion polymerizations are of the greatest interest.[8] The method, utilizing oil-in-oil (O/O),[9] water-in-oil (W/O), or oil-in-water (O/W) emulsions as flexible self-assembled templates, allows not only an easy preparation a large variety of polymeric capsules, but also permits a one-pot encapsulation of various guest species (adhesives, agrochemicals, biomolecules, flavors, fragrances, drugs, and dyes) during preparation of the capsules.[10]

Stimuli-responsive hollow hydrogel MCs offer even greater versatility for encapsulation and triggered release, which can be controlled by changing temperature, pH, ionic strength, or other stimuli.[11] Poly(*N*-isopropylacrylamide) (PNIPAM) hydrogels undergo a sharp volume transition near the lower critical solution temperature (LCST) from a highly hydrated swollen state below LCST to a dehydrated collapsed state above the LCST.[12] This effect is largely exploited in "smart" PNIPAM hydrogel MCs, in which a shell permeability is modulated by temperature. Most of PNIPAM hydrogel MCs were designed for, predominantly, biomedical needs to function in water environment and therefore, featured by hydrophilic outer surfaces.[13] However, for many other important applications, such as in catalysis, cosmetic, agrochemistry, or for smart coatings,[14] complex MCs having hydrophobic outer surfaces (to provide dispersibility in organic solvents) and hydrophilic interior for encapsulation of polar compounds, are also strongly desired. In this work we aimed at the preparation of such MCs. Hydrophilic and potentially thermoresponsive PNIPAM was chosen as a material for the preparation of capsules walls, and polyisoprene, as a hydrophobic corona-forming component.

Synthesis of PNIPAM MCs via the standard W/O emulsion polymerization using low molecular weight surfactants (e.g., Span 80) was previously reported.[13a] Although as-formed dispersions of these MCs were stable in the oil due to an excess of the Span 80 surfactant, subsequent purification of the MCs from the polymerization byproduct significantly reduced their colloidal stability in apolar solvents. In the present work, instead of easily removable small-molecule surfactants, we utilized polyethyleneoxide−polyisoprene block copolymer (PEO_{131}-*b*-PI_{361}) as macromolecular surfactant for W/O emulsion and prepared PNIPAM MCs that form stable dispersions in apolar solvents. Swelling behavior and encapsulated properties of the resulting MCs were preliminarily tested and the obtained results are reported herein.

Experimental Part

Instrumentation. Dynamic light scattering (DLS) measurements were performed by Zetasizer Nono S, (He−Ne-laser 4 mW, 632.8 nm, back scattering, NIBS-Technology, Malvern Instruments). Fluorescent images were obtained using an Axio Imager Microscope with 50X objective (Carl Zeiss, Jena, Germany). For data acquisition a filter set 15 (excitation, BP 546/2; beam splitter, FT 580; emission, LP 590) in conjunction with a SPOT Insight camera (Diagnostic instruments inc., Sterling Heights MI) and a MetaMorph imaging system (Molecular Devices, Downingtown, PA) were used. Scanning electron microscopy was carried out using Ultra 55 (Carl Zeiss SMT, Jena, Germany) operating at 3 kV in the secondary electron (SE) mode. TEM measurements were performed with Libra 200 (Carl Zeiss SMT). UV/vis measurements were carried out using Perkin-Elmer

*Corresponding author. E-mail: (V.S.) senkovskyy@ipfdd.de; (A.K.) kiriy@ipfdd.de.

Published on Web 06/24/2009

UV/vis spectrometer Lambda 800. ^{1}H NMR spectra were recorded on a Bruker DRX-500 spectrometer operating at 500.13 MHz for ^{1}H using $CDCl_3$ as solvent. The spectra were referenced on the solvent peak (δ(1H) = 7.26 ppm). GPC measurements were carried out on Agilent 1100 Series (Agilent) normal-temperature size exclusion chromatograph, equipped with refractive index detector and one column PL Gel MIXED-B (Polymer Laboratories, U.K.), eluent = chloroform, and flow rate of 1 mL/min. Calibration was based on polystyrene standards obtained from Polymer Standards Service (PSS, Germany). For AFM imaging NanoScope IV-D3100 (Digital Instruments, Santa Barbara, CA) was used. Imaging were performed with silicon tips with radius of 10−20 nm, spring constant of 30 N/m, and resonance frequency of 250−300 kHz.

Materials. Polyethyleneoxide-*block*-polyisoprene (PEO_{131}-*b*-PI_{361}) ($M_{n,PEO\text{-}b\text{-}PI}$ = 30 400 g/mol, $M_{w,PEO\text{-}b\text{-}PI}$ = 39 400 g/mol, $PDI_{PEO\text{-}b\text{-}PI}$ = 1.3; a parent PI_{361}, $M_{n,PI}$ = 24 600 g/mol, $M_{w\,PI}$ = 29 000 g/mol, PDI_{PI} = 1.18) was synthesized by anionic polymerization according to the previously published protocol.[15] All other chemicals were purchased from Aldrich and used as received.

Preparation of PNIPAM Microcapsules. First, 0.15 g of PEO_{131}-*b*-PI_{361} was dissolved in 3 mL of trimethylpentane (TMP), as the oil phase. Then, 0.15 g of *N*-isopropylacrylamide (NIPAM), 0.01 g (5 mol %) of methylenbisacrylamide (MBA), and 0.006 g of potassium persulphate (KPS) (1 mol %) were dissolved in 0.5 mL of deionized water, as the water phase. Water and oil phases were mixed in Ultra-Turax mixer (IKA, Germany) at 13500 rpm. The stirring was stopped after 2 min and the resulting emulsion was transferred into the glass tube equipped with magnetic stirrer. Temperature of the mixture was rapidly risen to 80 °C and the polymerization was carried out for 1 h. The excess of the surfactant was washed out by repeated centrifugation and redispersion in pure TMP. The resulting particles formed stable dispersions in cyclohexane, isooctane, anhydrous THF and in THF/water mixtures with water content up to 10%, but flocculated at higher water content. The MCs do not form stable dispersions in pure water and methanol.

Results and Discussions

To prepare PNIPAM microcapsules we performed W/O emulsion copolymerization of NIPAM and water-soluble cross-linker (MBA) in the presence of a water-soluble initiator (KPS) and PEO_{131}-*b*-PI_{361} block copolymer surfactant. An important prerequisite for the formation of the capsules in this method is that the polymerization was conducted at temperature above the LCST of PNIPAM that, we believe, induced precipitation of the formed phase-separated PNIPAM at the W/O interface.

Although the synthetic protocol used herein has many common features with earlier reported synthetic routes to similar microcapsules,[13] it has few important differences. Thus, Choi et al.[13b] reported preparation of PNIAPM microcapsules by polymerization of NIPAM at temperature below LCST of PNIPAM in a oil−water emulsion formed in a microfluidic device. To stabilize the capsulate morphology they utilized an oil-soluble initiator that decomposed by UV-light irradiation to give radicals in the oil phase. In that case, a portion of radicals coming from the oil phase and reached the interface with water was responsible for the initiation of the polymerization selectively from the interface. Sun et al.[13a] applied a combination of three factors to achieve the hollow morphology for PNIPAM particles. First, according to their method initiating radicals were induced selectively at the oil−water interface by diffusion and subsequent reaction of two precursors, the first one soluble in the oil, and the second one, in the water phase. Second, they used an oil-soluble cross-linker that, as expected, diffused from the oil phase into the water droplet and cross-linked NIPAM preferentially in a vicinity to the oil−water interface. Third, the polymerization was performed at temperature above LCST of PNIPAM at which formed PNIPAM is neither soluble in water nor in oil and may precipitate at the oil−water interface.

We found out that if the W/O polymerization of NIPAM is carried out at temperatures above the LCST of PNIPAM, the selective generation of radicals at the oil−water interface is unnecessary for achieving of hollow structures since the phase-separation of the forming cross-linked PNIPAM above the LCST is a sufficient factor to induce the formation of the microcapsules. Indeed, a distinct difference of our approach from the above-cited ones is that we do not apply any special measures to selectively generate initiating radicals at the oil−water interface and we do not promote stabilization of the hollow morphology inducing cross-linking selectively at the interface.

In our case, the monomer, the cross-linker, and the initiator used are soluble in water and are poorly soluble or not soluble in the oil. A partition of NIPAM and KPS between the water and the oil phases (in the absence of surfactants) was determined for two temperatures: (1) room temperature, i.e., temperature at which the emulsion for further polymerization was prepared, and (2) 80 °C, i.e., polymerization temperature. We found that a content of NIPAM in the oil phase is negligible at room temperature and it growth to about 20% as temperature rises up to 80 °C. The solubility of the KPS in the oil is negligible at both temperatures. Thus, it can be concluded that during the polymerization a major portion of the reactants is located in the water phase. It can be also assumed that at relatively high temperature used (80 °C) radicals are rapidly forming in the whole volume of the water droplets and thus the formation of the cross-linked PNIPAM is expected to occur in the whole volume of the droplets, and not only at the oil−water interface. If so, no formation of hollow spheres could be expected for polymerizations performed under such conditions if the formed polymer (e.g., polyacrylamide) is miscible in the dispersed phase (i.e., water). Indeed, a control experiment demonstrated that when more polar acrylamide instead of NIPAM is polymerized under otherwise the same polymerization conditions, nonhollow polyacrylamide hard microspheres are formed (Figure S1). Similar result could be expected for the polymerization of NIPAM below its LCST (using initiators with low decomposition temperatures). However, at temperatures above LCST of PNIPAM the polymerization of NIPAM in aqueous solutions proceeds differently and follows a so-called precipitation-polymerization mechanism. According to it, if the polymerization is carried out in water hydrophobic PNIPAM oligomers formed at early stages of the polymerization precipitate from the aqueous medium and aggregate to form nuclei that further grow finally resulting into well-defined PNIPAM microspheres.[16a] When the polymerization of NIPAM is performed in the presence of added template particles with an appropriate surface functionality, then the precipitation of the growing PNIPAM occurs selectively on the added particles (precipitation on convex surfaces).[16b] We suggest that similar mechanism occurs in our experiments with the only difference that the concave surfaces of the droplets featured by the macromolecular surfactant act here as seeds for selective precipitation of the phase-separated PNIPAM leading to the microcapsulate morphology. It is likely that formed hydrophobic NIPAM oligomers preferentially accumulate at the oil−water interface rather than homogeneously nucleate in water due to a higher hydrophobicity of the continuous phase and of the block copolymer surfactant than of the water. Phenomenologically, this process is similar to the process of the formation of polymeric microcapsules in O/W miniemulsions in detail described by McDonalds et al.[8a] and Landfester et al.[8b] In their cases, a hydrophobe and a monomer formed a common miniemulsion, whereas the formed polymer was immiscible with the hydrophobe and demixed throughout the polymerization to form the hollow

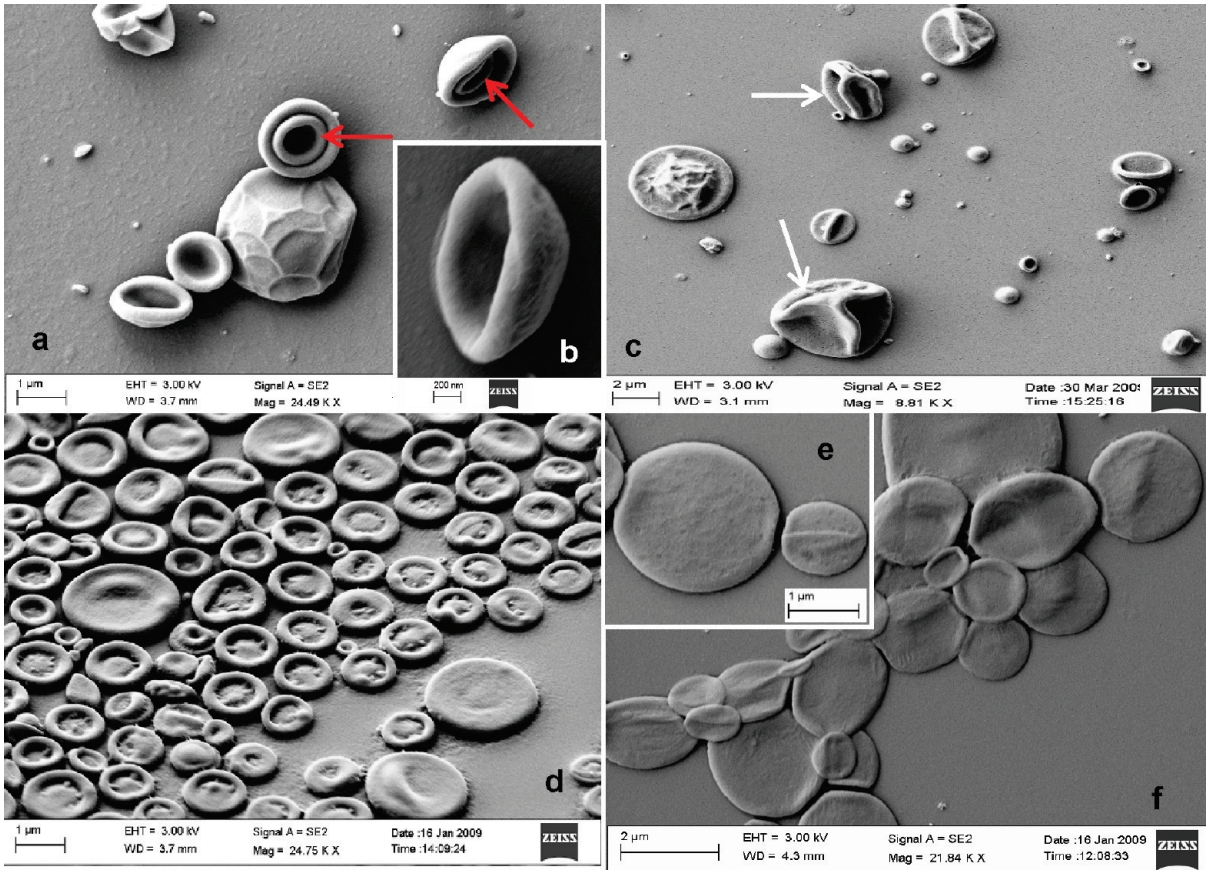

Figure 1. SEM images of the MCs deposited onto Si wafer: from a dispersion in cyclohexane (a−c); from a dispersion in THF (to get the information about the thickness of the structures, the imaging was performed for the sample tilted at 54°) (d); from a dispersion in THF/water (100/3 v/v) (e, f).

polymer structure surrounding the hydrophobe. The method developed in our work can be considered as an inverse-phase analogous of the process described by McDonalds et al. and Landfester et al.[8b] An important prerequisite for an efficient encapsulation of one immiscible liquid by another one both dispersed in a third immiscible liquid according to Torza et al.,[8c] is that relative surface tensions between the three phases must be in a correct order.[8] This rule is luckily satisfied in our case since the polarity of PNIPAM above LCST falls in between a highly apolar continuous phase (isooctane) and a highly polar disperse phase (water) and thus, the encapsulation of water by PNIAPM can be expected.

Another important difference from the earlier reported protocols is that we use the *macromolecular* surfactant that provides an efficient stabilization of the microcapsules in oils even after extensive purification of the microcapsules, thus demonstrating that the macromolecular surfactant is firmly attached to the microcapsules. The later effect is, most likely, due to a covalent cross-linking of the reactive PI block by radicals formed at the oil−water interface (that came from the water phase) upon NIPAM polymerization.

The hollow morphology of the resulting PNIPAM structures was detected by scanning electron, transmission electron, and atomic force microscopy (SEM, TEM, and AFM, respectively, Figure 1 and 2). On those images the microcapsules appear as Z-collapsed microstructures, 1−3 μm in a diameter, with either concave hemispherical (Figure 1a,b), or folded (Figure 1c), or toroidal (Figure 1d), or pancake (Figure 1e,f) morphologies, depending on the deposition conditions.[17]

Obviously, the final morphology of the MCs in the dry state depends on mechanical properties of the MCs walls in different solvents. The deposition from cyclohexane leads to less collapsed hemispherical (Figure 1a,b) and folded (e.g., marked by white arrows in Figure 1c) structures (these structures have larger heights compared to heights of the MCs deposited from other solvents). In cyclohexane the MCs walls possess, obviously, the highest mechanical strength among the solvents studied, since cyclohexane is a nonsolvent for PNIPAM that does not swell the MCs walls. Clear, such particles can be formed only from *hollow* microspheres upon their Z-collapse, as shown in Scheme 1, pathways i, ii, and iii.

The hollow structure of these hemispheres is further confirmed by the fact that in some cases smaller hemispheres are located inside the larger ones, as marked by red arrows in Figure 1a. These hemispheres are clearly different from ones formed upon the deposition of polyacryamide microspheres that for comparison shown in Figure S1 and Scheme 1, pathway vii. THF, which is a "good" solvent for PNIPAM, swells the MCs walls making them easily deformable. The deposition from THF results into much more flat structures compared to those formed from cyclohexane, but they still are not completely squashed (Figure 1d, Scheme 1, pathway iv). In this case, the toroidal morphology of the structures is given by the fact that the complete flattening of the MCs must derive rather strong deformation of the material near edges of the toroids, which, consequently, would require a much higher load than that needed to cause the collapse of central areas of the MCs. Finally, fully flat pancake structures are formed upon the deposition from THF/water mixture due to further softening of the PNIPAM walls in the aqueous solvent (Figure 1e,f and Scheme 1, pathway v). Scheme 1 summarizes possible collapse scenarios occurring upon the deposition of the microcapsules from different solvents. Scheme 1 (pathways vi and vii) also shows the possible morphologies of the surface structures formed upon Z-collapse of nonhollow spheres, such as

polyacrylamide particles (Figure S1). Obviously, most of the PNIPAM structures observed on the images Figure 1 would not be formed from *nonhollow* spheres further confirming successful preparation of microcapsules in this work.

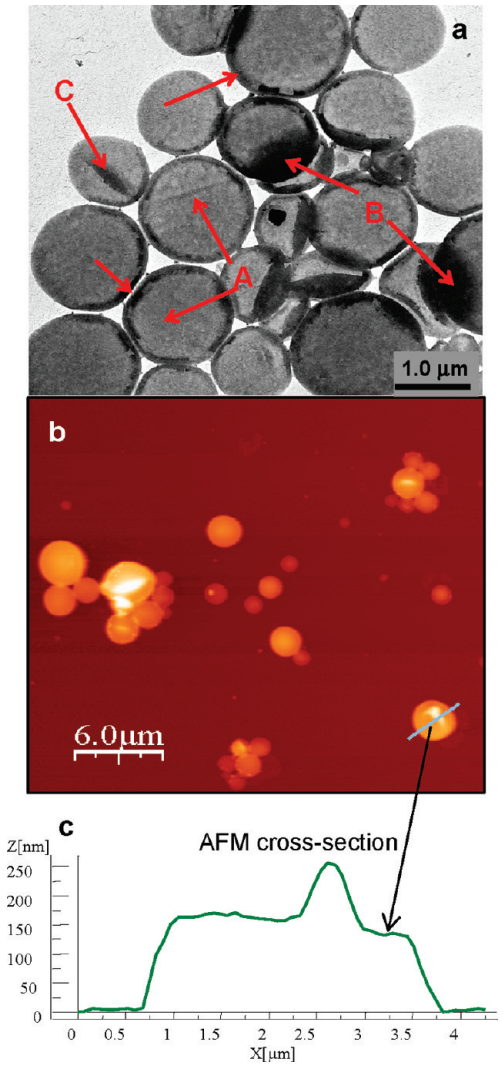

Figure 2. (a) TEM image of the MCs (see the text for the explanation). (b) AFM topography image of the MCs deposited on mica. (c) Cross-section of the AFM image performed along a line, as shown in part b.

TEM image of the microcapsules adsorbed onto amorphous carbon film is shown in Figure 2a. Areas with light-gray color (marked by arrows A) correspond to two-walls PNIPAM structures. Darker spots on the TEM image can be attributed to areas in which imaging electrons transmit through thicker PNIPAM layers. This happens (i) when the microspheres overlap one with another (arrows B), (ii) or when they fold (arrow C), (iii) or on curved edges of the toroid miscrospheres (arrows D) such as shown in Figure 1d and Scheme 1, pathway iv. The structures, that do not have darker edges can be attributed to fully flat pancake particles. Thus, TEM fully corroborates with the hollow morphology of the prepared PNIPAM microparticles, since the image of a nonhollow microsphere should be darker in the center of the sphere. AFM imaging (Figure 2b,c) reveals the expected pancake-like morphology. A cross-section of the AFM topography image gives a direct information about the thickness of double-wall structures (Figure 2c). Thus, a single-wall thickness of the MCs estimated from the images is about 150/2 = 75 nm, in a full agreement with the expected value for the water-to-monomers ratio used in the polymerization. It must be also emphasized that the PI shell that decorates the MCs and provides their stability in apolar solvents is not "seen" on the AFM images (on the SEM and TEM, as well), since it is too thin compared to the size of the MCs.[18]

The size of the MCs dispersed in different environment and temperatures was further investigated by dynamic light scattering (DLS). Freshly dispersed MCs in anhydrous THF show a hydrodynamic diameter of about 1 μm at room temperature (not shown). It gradually increases with time and reaches an equilibrium value of 1.8−1.9 μm upon the stirring for more than one day (Figure 3, black squares).

Most probably, such a long time to reach the constant size is needed for the MCs to restore the spherical shape from the collapsed hemispherical one. Addition of small amounts of water (i.e., 3−5% by volume) to the dispersion of the microcapsules equilibrated at room temperature in anhydrous THF moderately increases the size of the MCs up to 2.2 μm (Figure 3, red circles).[19] Further increase of the water content has a little influence on the MCs size; instead, they aggregate and precipitate, as the percentage of water exceeds the value of 10% (vol). The later effect is, likely, due to a strongly hydrophobic character of the outer polyisoprene surface that conflicts with the increased hydrophilicity of the environment.

Even higher swelling degrees were achieve using a tertiary THF/water/cyclohexane system as a dispersion medium. In control experiments we found that addition of cyclohexane to wet THF induces a stepwise phase-separation and precipitation

Scheme 1. (a) Structure of the PNIPAM Microcapsule (MCs) Having a Hydrophobic Polyisoprene Corona and (b) Morphologies for Collapsed Structures Possibly Formed upon Drying of Hollow and Non-Hollow Hydrogel Particles[a]

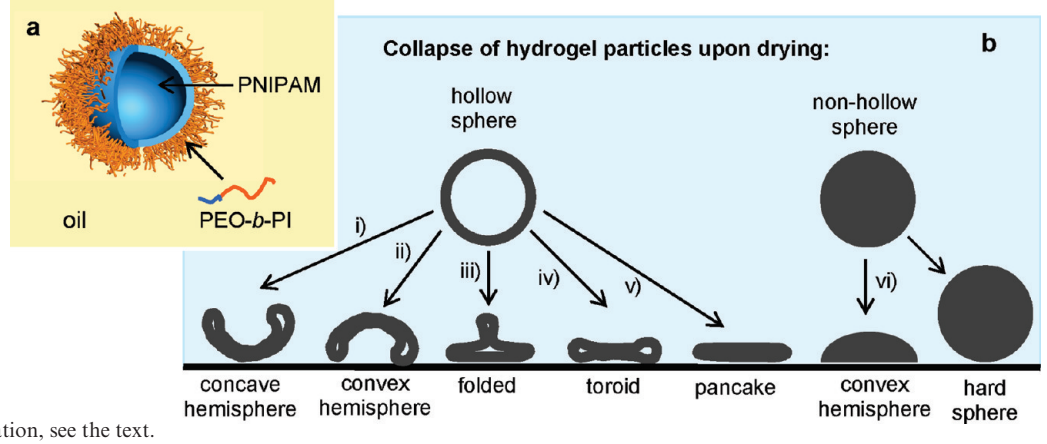

[a] For explanation, see the text.

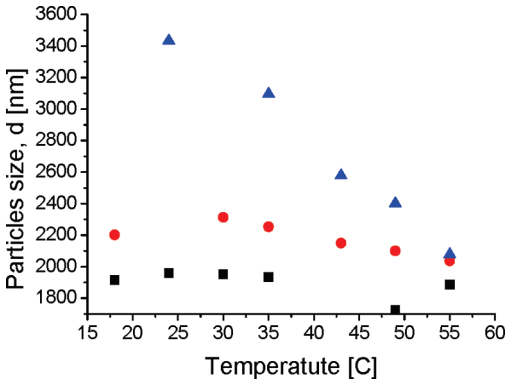

Figure 3. Dependence of the hydrodynamic diameter for the PNIPAM hydrogel MCs on temperature in different environments for MCs dispersed in: anhydrous THF (black squares); THF containing 3% of water (red circles); THF/water/cyclohexane mixture, 100/3/10 (blue triangles).

of a water-rich phase. Particularly, the initially clear THF/water solution containing 1 mL of THF and 30 μL of water becomes turbid after the addition of 150 μL of cyclohexane; the addition of 250 μL of cyclohexane derives a precipitation of ~5 μL of the water-rich phase that consist of ~90% of water and ~10% of THF (the content of cyclohexane in this phase is negligibly small). Simple calculations show that ~15% of the whole amount of water precipitates at this point (~85% of water still remains in the THF-rich phase). The phase-separation reaches its maximum upon addition of 600 μL of cyclohexane and ~21 μL of the water-rich phase precipitates. We assumed that if a similar experiment will be performed in the presence of MCs, the phase-separating water would enter the hydrophilic interior of the MCs, inducing an additional swelling of the MCs. To verify this hypothesis, a series of experiments were conducted directly in a cuvette for DLS measurements.

In a typical experiment, 100 μL of cyclohexane was added dropwise, or in a single portion, to the sample containing 0.5 mg of the MCs dispersed in 1 mL of THF and 30 μL of water. The DLS measurements were started in about 10 min after the cyclohexane addition, as soon as the dispersions recovered their initial appearance (the dispersions became a bit more turbid right after the addition of cyclohexane). The DLS measurements showed that the hydrodynamic diameter of the MCs increases up to 2.8−3.5 μm in these experiments (Figure 3, blue triangles). Hence, it is indeed possible to reach much higher swelling degrees for the MCs in the tertiary THF/water/cyclohexane system than those achievable in binary THF/water mixtures. The diameter of the MCs swollen in the tertiary solvent mixture was found to be dependent on particular mixing conditions (rate of cyclohexane addition, stirring intensity, etc.). Rather fast addition of cyclohexane, generally, favors achieving of higher swelling degrees of the MCs, than the slow addition. A reason of a poor reproducibility of the swelling result is not fully understood, however, we tentatively ascribe it to a complex nature of processes occurring in these experiments. Indeed, addition of cyclohexane to the THF/water mixture induces significant rearrangements in the system: a substantial portion of THF molecules that before addition of cyclohexane was solely involved in the solvation of water, is now consumed for interactions with a highly apolar cyclohexane. As a result, water molecules are no more efficiently solvated due to increased hydrophobisity of the solvent mixture and phase-separate onto the water-rich and water-poor phases. The water-rich phase has two alternative pathways to release hydrophobic surrounding: either to aggregate into macroscopic droplets and precipitate, or to enter into the hydrophilic interior of the MCs. This uncertainty might explain a poor reproducibility of the swelling process. The later pathway is associated with additional energetic barriers required for diffusion of polar water molecules through the apolar polyisoprene shell and for the penetration of the PNIPAM wall. An exact segregation scenario, i.e., what fraction of the water-rich phase will follow the first segregation pathway and what (the second one) is a complex function of many factors (e.g., rate of cyclohexane addition, stirring intensity, temperature, etc.), not all of which are easily controllable or even known. Therefore, more investigations are necessary to shed a light on this process.

A practically important feature of the PNIPAM-based objects is their thermoresponsiveness, the property inherently associated with the interaction of PNIPAM with water. Our experiments deal with the solvent containing minute amounts of water (i.e., 3%) and thus, from the first sight, thermo-driven phase transitions of PNIPAM are unlikely here. Indeed, although the phase transition of PNIPAM occurs in THF/water mixtures[20] and in other mixed aqueous solutions (cononsolvency effects),[21] a substantial fraction of water in the mixed solutions is needed to ensure the thermoresponsiveness. For example, in the THF/water mixtures PNIPAM exhibits the LCST, if the water content exceeds a value of 35%, whereas THF-rich mixtures (water content < 35%) are good solvents for PNIPAM.[20]

Figure 3 shows dependencies of the hydrodynamic diameter of our MCs in different environment at different temperatures, measured by DLS. As expected, in anhydrous THF (Figure 3, black squares) and in THF/water mixtures (Figure 3, red circles) the size of the MCs remains almost constant within the experimental error in the temperature interval from 17 to 55 °C. In contrast, the size of the MCs in the tertiary THF/water/cyclohexane system is temperature-dependent. The most pronounced changes in the MCs size were observed for highly swollen MCs with the diameter of 3.5 μm obtained upon the fast addition of cyclohexane to the MCs dispersion in THF/water mixture (Figure 3, blue triangles). In this case, the rise of the temperature from 23 °C up to 55 °C induces continuous deswelling of the MCs to the diameter of 2 μm, that is close to the MCs size in anhydrous THF. Cooling of this dispersion down to the room temperature induces reswelling of the MCs up to 3.5−3.7 μm (not shown).

Although the overall content of water in the system (i.e., 3%) is too low to ascribe the observed changes of the MCs size to the conventional temperature-driven phase transition of PNIPAM, after addition of cyclohexane the water-rich phase is allocated preferentially inside the MCs (water content in this phase is ~90%). Hence, water phase directly interacts with the inner surface of the PNIPAM wall and can efficiently hydrate it. From these considerations the temperature-driven phase transition of PNIPAM in the investigating system looks feasible. In this case, the PNIPAM walls dehydrate and tend to shrink, as soon as temperature rises above 35 °C. At the same time, the outside part of the MCs wall is in a contact with the THF-rich part and, hence, the walls can be reswollen with THF as soon as PNIPAM becomes dehydrated. Thus, the process occurring upon increase of temperature in this system phenomenologically can ascribed to the transition of PNIPAM from the swollen-in-water to the swollen-in-THF states[22] rather than to the conventional coil-to-globule transition. The PNIPAM wall softened by THF, becomes more penetrable for solvents that facilitates the release of the water-rich phase from the MCs interior and their deswelling down to the size inherent to the swollen-in-THF MCs (i.e., ~2 μm).

However, there is also an additional factor that further complicates the situation. We found that the increase of the temperature significantly enhances solubility of water in the THF/cyclohexane mixture so that a predominant quantity of water segregated at room temperature upon the addition of cyclohexane, could be then redissolved at increased temperature. If so, an

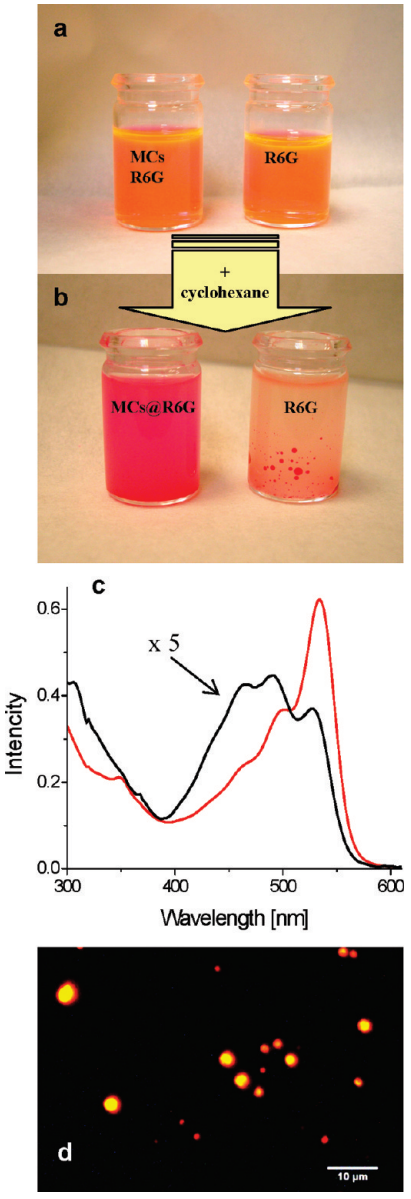

Figure 4. (a) Photographs of Rhodamin 6G dissolved at the concentration of 0.01% in THF containing 1% of water in the presence of the MCs (0.1%, left) and in the absence of the MCs (right). (b) Same samples after the addition of cyclohexane. (c) UV−vis absorption spectra: of the left-hand sample in part b (red line); and of the right-hand sample in part b (black line). (d) Fluorescent micrograph of the MCs loaded with Rhodamine 6G solution dispersed in an non-volatile oil.

increased solubility of water in the "hot" solvent mixture very likely causes its uptake from the MCs. Thus, both these effects might contribute to the observed thermo-driven reversible swelling/deswelling of the MCs.

Encapsulating properties of the PNIPAM hydrogel microcapsules were preliminarily studied using Rhodamin B (R6G) dye as a model compound. The above-described procedure for the swelling of the MCs in the tertiary THF/water/cyclohexane system was applied for loading of the MCs. At first, we examined a behavior of R6G at different solvent compositions by adding the solution of R6G in water (1%) to anhydrous THF. It was found that at the concentration of R6G used, it does not precipitate from wet THF if the water fraction exceeds 1% (Figure 4a, right-hand sample), although the solubility of R6G in THF/cyclohexane mixtures is poor. Thus, an addition of cyclohexane to the solution of R6G in the THF/water mixture results in segregation and precipitation of the water-rich phase that accumulates the main quantity of R6G (Figure 4b, right-hand sample). Significantly blue-shifted structured and of a lowered intensity UV−vis spectrum of the supernatant reveals that R6G is present in a strongly aggregated form (Figure 4c, black line, the signal was multiplied factor of 5).

To load the microcapsules with R6G solution, 10 μL of the R6G solution in water (1%) was added to the dispersion of the MCs (1 μg) in the mixture of 1 mL of THF and 10 μL of water (Figure 4a, left-hand sample).

Since the amount of the microcapsules in the dispersion is rather small, a predominant quantity of R6G at this stage is located in the dispersion medium. Addition of 100 μL of cyclohexane to this dispersion induces the encapsulation of a major fraction of the water phase containing R6G is into the MCs (MCs@R6G) forming a stable colloidal dispersion of encapsulated R6G (Figure 4b, left-hand sample). This observation is in a sharp contrast with the above-described experiment performed in the absence of the MCs when the addition of cyclohexane resulted into near complete precipitation of R6G. The obtained MCs and R6G dispersion exhibits UV−vis absorption spectrum typical for R6G molecularly dissolved in water-rich solvent mixtures (Figure 4c, red line). The MCs loaded with R6G solution appear on the fluorescent microscopy images, as strongly fluorescent objects, 2.5−3.5 μm in diameter, in an agreement with DLS measurements. As seen from the Figure 4d, R6G is homogeneously distributed inside the MCs, rather than segregated in the MCs walls or located outside the MCs.

Conclusions

PNIPAM hydrogel microcapsules having a hydrophobic corona were prepared by a water-in-oil emulsion polymerization using polyethyleneoxide-polyisoprene block copolymer as the corona-forming compound. A hollow morphology of the microcapsules is provided by the precipitation−polymerization mechanism where water/oil interface of the W/O emulsion acted as soft templates and seeds that induce selective precipitation of PNIPAM above its LCST. The developed method does not require any potentially toxic additives for generation of initiating radicals at the water/oil interface and this would be important for biomedical applications of the MCs. The resulting hydrogel microcapsules form stable dispersions even in highly apolar organic solvents, such as cyclohexane, but rapidly flocculate in water. It is noteworthy that the hydrogel MCs loaded with water solutions show a well-pronounced swelling/deswelling transition triggered by temperature in THF that contains only minute amounts of water. An approach to efficiently load the microcapsules with aqueous solutions, based on addition of aqueous solutions to the dispersion of the microcapsules in THF followed by addition of apolar solvents to induce the segregation of the water phase, was developed. The shell of the microcapsules was found to be permeable for water-soluble molecules (e.g., Rhodamine 6G) and hence, the microcapsules can be envisaged for applications that require controlled dispersions and release of hydrophilic species in an oil environment.

Acknowledgment. We thank Dr. Peter Formanek for TEM measurements. Financial support was provided by the Deutsche Forschungsgemeinschaft (STA 324/32-1, SPP 1259/1 "Intelligente Hydrogele").

Supporting Information Available: SEM image of polyacrylamide microspheres. This material is available free of charge via the Internet at http://pubs.acs.org.

References and Notes

(1) Thies, C. In *Drugs and the Pharmaceutical Sciences*; Benita, S., Ed.; Marcel Dekker: New York, 1996; *Vol*. 73.

(2) Chen, C. W.; Chen, M. Q.; Serizawa, T.; Akashi, M. *Chem. Commun*. **1998**, 831–832.

(3) Hoare, T.; Pelton, R. *Macromolecules* **2007**, *40*, 670–678.

(4) (a) Das, M.; Zhang, H.; Kumacheva, E. *Annu. Rev. Mater. Res*. **2006**, *36*, 117–142. (b) Suzuki, D.; McGrath, J. G.; Kawaguchi, H.; Lyon, L. A. *J. Phys. Chem. C* **2007**, *111*, 5667–5672.

(5) (a) Tamber, H.; Johansen, P.; Merkle, H. P.; Gander, B. *Adv. Drug Delivery Rev*. **2005**, *57*, 357–376. (b) Hammer, D. A.; Discher, D. E. *Annu. Rev. Mater. Sci*. **2001**, *31*, 387–404.

(6) (a) Caruso, F.; Caruso, R. A.; Mohwald, H. *Science* **1998**, *282*, 1111–1114. (b) Donath, E.; Sukhorukov, G. B.; Caruso, F.; Davis, S. *Angew. Chem Int Ed* **1998**, *37*, 2202. (c) Johnson, S. A.; Ollivier, P. J.; Mallouk, T. E. *Science* **1999**, *283*, 963–965. (d) Bronich, T. K.; Ouyang, M.; Kabanov, V. A.; Eisenberg, A.; Szoka, F. C.Jr; Kabanov, A. V. *J. Am. Chem. Soc*. **2002**, *124*, 11872–11873.

(7) (a) Dowding, P. J.; Atkin, R.; Vincent, B.; Bouillot, P. *Langmuir* **2004**, *20*, 11374. (b) Dinsmore, A. D.; Mink, F.; Hsu, M. G.; Marques, M.; Bausch, A. R.; Weitz, D. A. *Science* **2002**, *298*, 1006. (c) Hotz, J.; Meier, W. *Langmuir* **1998**, *14*, 1031. (d) Qian, J.; Wu, F. P. *Chem. Mater*. **2007**, *19*, 5839–41. (e) Peyratout, C. S.; Dahne, L. *Angew. Chem., Int. Ed*. **2004**, *43*, 3762. (f) Velev, O. D.; Furusawa, K. *Langmuir* **1996**, *12*, 2374. (g) Chu, L. Y.; Xie, R.; Zhu, J. H.; Chen, W. M.; Yamaguchi, T.; Nakao, S. *J. Colloid Interface Sci*. **2003**, *265*, 187. (h) Nakagawa, K.; Iwamoto, S.; Nakajima, M.; Shono, A.; Satoh, K. *J. Colloid Interface Sci*. **2004**, *278*, 198.

(8) (a) McDonald, C. J.; Bouck, K. J.; Chaput, A. B.; Stevens, C. J. *Macromolecules* **2000**, *33*, 1593–1605. (b) Tiarks, F.; Landfester, K.; Antonietti, M. *Langmuir* **2001**, *17*, 908–918. (c) Torza, S.; Mason, S. G. *J. Colloid Interface Sci*. **1970**, *33*, 6783.

(9) Kobaslija, M.; McQuade, D. T. *Macromolecules* **2006**, *39*, 6371–6375.

(10) Crespy, D.; Stark, M.; Hoffmann-Richter, C.; Ziener, U.; Landfester, K. *Macromolecules* **2007**, *40*, 3122–3135.

(11) Wie, W.; Zhang, C.; Ding, S.; Qu, X.; Liu, J.; Yang, Z. *Colloid Polym. Sci*. **2008**, *286*, 881–888.

(12) (a) Heskins, M.; Guillet, J. E. *J. Macromol. Sci*. **1968**, *A2*, 1441. (b) Hirotsu, S. *J. Chem. Phys*. **1988**, *88*, 427.

(13) (a) Choi, C.-H.; Jung, J.-H.; Kim, D.-W.; Chung, Y.-M.; Lee, C.-S. *Lab Chip* **2008**, *8*, 1544–1551. (b) Sun, Q.; Deng, Y. *J. Am. Chem. Soc*. **2005**, *127*, 8274–8275.

(14) Our group is developing smart coatings with inverse-switching behavior based on hydrogel microparticles: http://spp-hydrogele.bci.uni-dortmund.de/Stamm.html.

(15) Schmalz, H.; Knoll, A.; Müller, A. J.; Abetz, V. *Macromolecules* **2002**, *35*, 10004–10013.

(16) (a) McPhee, W.; Tam, K. C.; Pelton, R. H. *J. Colloid Interface Sci*. **1993**, *156*, 24–30. (b) Zha, L. S.; Zhang, Y.; Yang, W. L.; Fu, S. K. *Adv. Mater*. **2002**, *14*, 1090–1092.

(17) Similar hemispherical morphology was earlier observed for other microcapsules in the dry state: Koo, H. Y.; Chang, S. T.; Choi, W. S.; Park, J.-H.; Kim, D.-Y.; Velev, O. D. *Chem. Mater*. **2006**, *18*, 3308–3313.

(18) Shells (or coronas) around particles could be resolved with AMF for much smaller nanostructures such as micelles or star-like polymers in which the core and the shell are of comparable size: (a) Gorodyska, G.; Kiriy, A.; Minko, S.; Tsitsilianis, C.; Stamm, M. *Nano Lett*. **2003**, *3*, 365–368. (b) Kiriy, A.; Gorodyska, G.; Minko, S.; Tsitsilianis, C.; Stamm, M. *Macromolecules* **2003**, *36*, 8704–8711. (c) Sfika, V.; Tsitsilianis, C.; Kiriy, A.; Gorodyska, G.; Stamm, M. *Macromolecules* **2004**, *37*, 9551–9560.

(19) In pure water PNIPAM chains are somewhat stiffer than in organic solvents, such as in methanol: Fujishige, S. *Polym. J*. **1987**, *19*, 297 and references therein.

(20) Winnik, F. M.; Ottaviani, M. F.; Bossmann, S. H.; Pan, W.; Garcia-Garibay, M.; Turro, N. J. *Macromolecules* **1993**, *26*, 4577–85.

(21) (a) Wolf, B. A.; Willms, M. M. *Makromol. Chem*. **1978**, *179*, 2265. (b) Nandi, A. K.; Sen, U. K.; Bhattacharyya, S. N.; Mandel, B. M. *Eur. Polym. J*. **1983**, *19*, 283. (c) Horta, A.; Fernandez-Pierola, I. *Polym. Bull*. **1980**, *3*, 273. (d) Schild, H. G.; Muthukumar, M.; Tirrell, D. A. *Macromolecules* **1991**, *24*, 948.

(22) (a) Zhang, X.-Z.; Chu, C.-C. *Colloid Polym. Sci*. **2004**, *282*, 589–595. (b) Pagonis, K.; Bokias, G. *Polym. Bull*. **2007**, *58*, 289–294.